

# Transparent Transmission of a Secure Time Domain Spectral Phase Encoding/Decoding DPSK–OCDM Signal Over a DWDM Network

Zhensen Gao, Bo Dai, Xu Wang, Nobuyuki Kataoka, and Naoya Wada

**Abstract**—We propose and experimentally demonstrate a transparent optical-code-division multiplexing (OCDM) overlay public dense wavelength-division multiplexing (DWDM) network architecture enabled by a passive spectral notch filter for extracting and detecting a secure OCDM signal, which employs a time domain spectral phase encoding/decoding scheme that can simultaneously generate differential-phase-shift-keying (DPSK) data and optical code patterns using only a single phase modulator. The time domain encoded OCDM signal has been scrambled bit-by-bit by a prime hopping pattern and concealed in the public DWDM channels to significantly improve the OCDM channel security. The effect of optical code patterns, the channel number, and bandwidth of the spectral notch filters on the system performance has been theoretically simulated and experimentally validated. In the experiment, error-free transmission of a 2.5-Gb/s time domain spectral phase encoded DPSK–OCDM signal with three 8-chip, 20-Gchip/s optical codes and a scrambled code pattern in the transparent OCDM overlay two-channel 10-Gb/s DWDM network has been successfully demonstrated.

**Index Terms**—Fiber optics and optical communications; Multiplexing; Optical-code-division multiple access; Phase modulation.

## I. INTRODUCTION

Fiber-optic communication has evolved over the past decades as an attractive technology to offer high bit-rate transmission and tremendous bandwidth. In the deployment of a modern fiber-optic communication network, secure data exchange is receiving increasing attention for both military and commercial applications. Achieving high data security is a challenge for future broadband all-optical networks. Optical-code-division multiple access (OCDMA) is considered as one of the promising technologies for providing intrinsic data confidentiality [1–4] because, in an OCDMA system, the data presents as a noise-like signal after optical encoding that

is barely interceptable by the eavesdropper without knowing the applied optical code.

On the other hand, to meet the explosive growing capacity demand of the fiber-optic network, efficient utilization of the limited bandwidth is particularly important [5]. Wavelength-division multiplexing (WDM) has already been demonstrated as an effective technique to increase the bandwidth efficiency [6]. In the WDM network, the data is transmitted over multiple carrier wavelengths, which are kept far apart to avoid the crosstalk between different channels. Dense WDM (DWDM) can efficiently exploit the bandwidth and has been widely deployed in the current fiber-optic infrastructure.

A method of overlaying the optical-code-division multiplexing (OCDM) channel on an existing public DWDM network may be a prospective solution to improve both the system security and bandwidth efficiency. In an OCDM overlay DWDM system, the usable channels can be significantly expanded in two dimensions [7]: wavelength and code. It is possible to make full use of the broadband spectrum between the DWDM grids through spectrally overlaying the OCDM channel onto the public DWDM network and simultaneously processing the OCDM and DWDM signals during the transmission by using the same erbium-doped fiber amplifier (EDFA) to increase the bandwidth efficiency, system flexibility, and energy efficiency. Efforts have already been made to demonstrate this capability by overlaying the OCDM channel on a public WDM channel [8–11]. Meanwhile, the OCDM overlay DWDM system can also provide an additional level of security that can supplement the optical encoding. Previously, it has been demonstrated that by using chromatic dispersion to stretch the data pulse such that its peak amplitude is reduced to a very low level comparable to the system noise, the data pulse can be concealed underneath an existing public channel to achieve physical layer security [12–14]. By combining the chromatic dispersion based approach with the optical coding technique, one can spectrally overlay a broadband, low power density OCDM signal on the public DWDM channels to avoid the attention of the OCDM channel and improve the data confidentiality.

Because the spectrum of the OCDM and DWDM signal occupies the same spectral band, the main issue in the network is to correctly recover the secure OCDM data from the hybrid signals. Optical thresholding and time gating techniques [8,12]

Manuscript received November 15, 2010; revised February 10, 2011; accepted March 4, 2011; published April 14, 2011 (Doc. ID 138063).

Zhensen Gao, Bo Dai, and Xu Wang (e-mail: x.wang@hw.ac.uk) are with the Joint Research Institute for Integrated Systems, School of Engineering and Physical Sciences, Heriot-Watt University, Edinburgh, EH14 4AS, UK.

Nobuyuki Kataoka and Naoya Wada are with the National Institute of Information and Communications Technology (NICT), Koganei, Tokyo, 184-8795, Japan.

Digital Object Identifier 10.1364/JOCN.3.000404

have been employed to suppress the interference of the WDM signal. To simplify the OCDM detection, a spectral notch filter has been proposed to directly reject the public channel interference in a temporal phase encoded time spreading (TS) OCDM system [15]. Transmission of a stealth amplitude modulated signal over a public differential-phase-shift-keying (DPSK) link has also been demonstrated by using a spectral notch filter [16]. However, up to now, only the on-off-keying (OOK) data modulation format for the stealth channel has been reported in the OCDM overlay public WDM system, which may not satisfy the indispensable requirement of network transparency for future all-optical networks. A transparent all-optical network should be able to support versatile advanced optical modulation formats, bit rate, and protocols [17]. While the network transparency can enable a low cost, power efficient, highly flexible, and scalable all-optical network, the implementation of the OCDM channel over the public DWDM network should also be compatible with this transparent environment by supporting various modulation formats, optical en/decoding schemes, and detecting the OCDM signal without inducing any additional architecture requirement and impairment of the existing public channel. By using a simple passive spectral notch filter in the OCDM overlay DWDM system, the network transparency could be achieved while the security of the OCDM channel can also be guaranteed in either a coherent TS-OCDM or spectral phase encoding time spreading (SPECTS) OCDM system. Recently, we proposed a novel time domain spectral phase en/decoding (SPE/SPD) scheme with the unique feature of rapid reconfigurability for OCDM applications [18]. In contrast to conventional en/decoding techniques, the time domain SPE/SPD scheme can simultaneously generate spectral phase en/decoding and DPSK data modulation to simplify the system architecture and reduce the cost. It can also support bit-by-bit optical encoding with the DPSK data to significantly enhance the security of the OCDM channel.

In this paper, we experimentally demonstrate the transparent transmission and detection of a secure 2.5-Gb/s time domain spectral phase encoded OCDM signal with the DPSK modulation format spectrally overlaid on a two-channel 10-Gb/s DWDM network without any complicated optical thresholding/time gating techniques. The DPSK-OCDM channel has been secured by both the time domain bit-by-bit spectral phase encoding and the public DWDM network. A fiber Bragg grating based spectral notch filter is employed for the network transparency. Error-free transmission of the 2.5-Gb/s DPSK-OCDM signal and the two-channel 10-Gb/s DWDM signal over 49 km of fiber has been successfully achieved.

## II. PRINCIPLE OF THE PROPOSED TRANSPARENT TIME DOMAIN SPE/SPD-OCDM/DWDM OPTICAL NETWORK

### A. Transparent OCDM/DWDM Network

Figure 1 shows the schematic diagram of the proposed OCDM overlay public DWDM network. In this architecture, the multi-channel DWDM signals are generated individually by different laser diodes and multiplexed by the optical multiplexer, whereas the secure OCDM signal, encoded by a

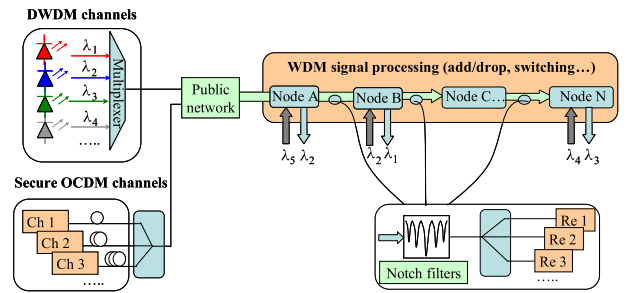


Fig. 1. (Color online) Schematic diagram of the proposed transparent secure OCDM channel over a public DWDM network.

different optical encoder for each channel and combined by a power combiner, is injected into the public network together with the DWDM signals. As the OCDM signal manifests itself as a noise-like signal after encoding, security enhancement can be achieved via spectrally overlaying the OCDM channel onto the public multi-channel DWDM network. With the introduction of high power public DWDM channels, it becomes more difficult for an eavesdropper to detect and intercept the secure OCDM channel. Compared with the previous architectures, which need complicated optical thresholding or time gating [8,12] to suppress the interference arising from the public channel and recover the OCDM signal before any DWDM signal processing (such as add-drop, wavelength conversion, optical switching, and regeneration), the proposed scheme enables extraction of the OCDM signal from the spectrally overlapped hybrid OCDM/DWDM signals by similarly using a low cost, passive spectral notch filter [15,16]. After inserting the passive spectral notch filter into the public network, all the DWDM channels can be rejected and directly transmit through the notch filters with negligible deterioration if the power ratio is high enough, while the encoded OCDM signal will be dropped down for the following decoding and detection.

Thanks to the adoption of spectral notch filtering, this architecture not only excludes the utilization of optical thresholding/time gating techniques, but also can support versatile advanced modulation formats such as OOK, DPSK, and differential-quadrature-phase-shift-keying (DQPSK), etc. It can also enable various optical encoding schemes (TS-OCDM and SPECT-OCDM) and detection of the OCDM signal at any point (before or after each network node) during its transmission throughout the whole network. Because the spectral notch filter can directly reject the DWDM interference, a high power ratio between the DWDM and OCDM signal can be anticipated while maintaining excellent system performance. The existence and architecture of the public DWDM channel is completely independent of the secure OCDM channel, and thus, the proposed OCDM overlay DWDM network can be fully transparent and enable secure OCDM transmission with various modulation formats.

### B. Time Domain Spectral Phase Encoding/Decoding

In a SPECTS-OCDMA system, the optical encoding is realized by applying a different phase shift to different spectral

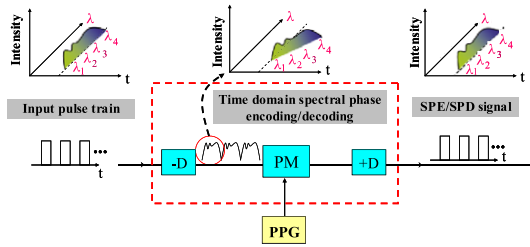


Fig. 2. (Color online) Operation principle of time domain SPE/D-OCDMA.

components of an ultrashort optical pulse, resulting in time spreading of the short pulse, whereas the decoding performs inverted phase changes on the corresponding spectral components by the proper decoder with a complementary phase shift pattern compared with that of the encoder. After the decoding, the phase of the resulting spectrum is frequency invariant, and therefore, the noisy pulse is temporally spread back to the original pulse shape [19]. The decoding performance for conventional spectral phase encoders/decoders is extremely sensitive to the wavelength drift of the laser source. However, the proposed time domain SPE scheme has the unique advantages of good compatibility, flexibility, and more importantly, it can relax the wavelength stability requirement and rapidly reconfigure the optical code.

Figure 2 briefly shows the schematic diagram of the reconfigurable time domain SPE/SPD scheme [18]. The SPE section is composed of a pair of dispersive devices with opposite dispersion values ( $-D$  and  $+D$ ) and a high speed phase modulator (PM). The ultrashort optical pulses with a broadband spectrum are generated from the pulse generator and directed into the first dispersive device ( $-D$ ) to stretch the pulse in the time domain, so that different spectral components of the signal spread at different positions in one bit duration. The PM is driven by optical code (OC) patterns to modulate the phases of different spectral components. The second dispersive component with a dispersion value of  $+D$  (opposite to the first one) compresses the encoded signal and generates a SPE signal. The SPE signal generated in this way can be decoded either by conventional spectral phase decoders or a similar time domain spectral phase decoding (SPD) configuration. In this scheme, any wavelength drift of the laser source will be converted into timing error, which is very easy to compensate for by adjusting an optical delay line. Moreover, the optical code is directly generated from the pulse pattern generator, so it can be rapidly reconfigured. By using only a single phase modulator, simultaneous DPSK data modulation and optical code generation can be achieved to simplify the architecture and reduce the cost. It is even possible to perform bit-by-bit code scrambling and DPSK data modulation to improve the OCDM security [20].

### III. EXPERIMENTAL DEMONSTRATION AND SIMULATION

Figure 3 illustrates the experimental setup to demonstrate the proposed hybrid network. The top left is the WDM transmitter, which consists of two-channel non-return-to-zero

(NRZ) OOK signals that are generated by two independent CW lasers spectrally centered at 1550.52 nm and 1551.32 nm and then modulated by an intensity modulator driven by a 10-Gb/s pseudo-random bit sequence (PRBS) of length  $2^{31} - 1$ . To generate the 2.5-Gb/s OCDM signal, an active mode-locked laser (MLL) producing nearly transform-limited 2.8 ps pulses at a repetition rate of 10 GHz and spectrally centered at 1549.9 nm is used as the laser source. The pulse train generated from the MLL is directed into an EDFA and a piece of 2 km dispersion-flattened fiber (DFF) for super-continuum (SC) generation in order to broaden the spectrum. The source repetition rate is then converted to 2.5 GHz by another intensity modulator. After that, a linearly chirped fiber Bragg grating (LCFBG) based dispersive element centered at 1550 nm is used to stretch the input pulse for spectral phase encoding. The 20-dB bandwidth and chromatic dispersion of the LCFBG are around 4.7 nm and  $-80$  ps/nm, respectively. Each bit of the original pulse will be stretched to  $\sim 376$  ps after the LCFBG. A single high speed PM driven by a pulse pattern generator (PPG) is employed to simultaneously generate the 2.5-Gb/s DPSK data mixed with 8-chip, 20-Gb/s optical code. An optical delay line is used before the phase modulator to temporally align the spectral phase code and the corresponding spectral component for each stretched pulse. After that, the OCDM signal is combined with the DWDM signal via a 3-dB coupler and then launched into a span of 49 km of dispersion-compensated transmission fiber.

In the receiver side, a fiber Bragg grating (FBG) based spectral notch filter with a center wavelength of 1550.9 nm and 10-dB bandwidth of 1 nm is used to emulate the transparent optical network, from which the two DWDM signals can be simultaneously dropped from the reflection port of the notch filter, distinguished by a 0.6 nm optical bandpass filter and finally detected by a 10-Gb/s optical packet receiver, which is composed of a photo-detector, an electrical amplifier, and a 10-Gb/s clock and data recovery circuit. After the drop operation of the DWDM signals, the OCDM output from the transmission port of the notch filter still remains and can be decoded using a configuration similar to the encoding part but with another PM driven by only the complementary code pattern sequence. Another LCFBG with opposite dispersion of  $+80$  ps/nm is used to compress the spectrally phase decoded pulse to recover the original data. The decoded signal is then directed into a 2.5-Gb/s DPSK demodulator followed by a balanced photo-detector (BPD) and an error detector to measure the bit error rate (BER).

To investigate the signal distortion after decoding and the resultant performance degradation due to the introduction of the spectral notch filter in the OCDM signal, we have theoretically simulated the effect of notch filtering on the spectrum and recovered waveform using the commercially available software OptiSystem 7.0. Figures 4(a)–4(d) show the encoded spectra after four different notch filters: (i) without a filter, (ii) one filter with a center wavelength of 1550.9 nm and bandwidth (BW) of 1 nm (used in this experiment), (iii) five 0.2 nm BW filters in accordance with the DWDM ITU-T grid with a channel spacing (CS) of 0.8 nm, and (iv) fifteen 0.2 nm BW filters for more dense WDM with a CS of 0.3 nm. The corresponding waveforms after decoding are shown in Figs. 4(e)–4(h), from which one can see that, compared to the case without a filter, the 1 nm bandwidth filter has cut nearly

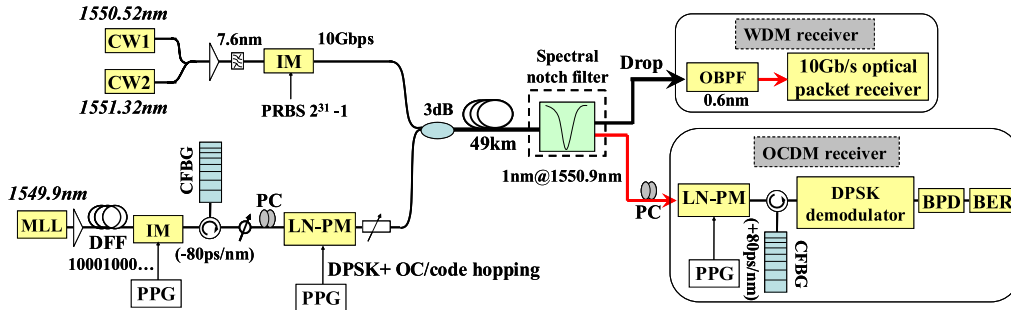


Fig. 3. (Color online) Experimental setup of the proposed time domain SPE/SPD-OCDM system spectrally overlaid on a two-channel DWDM network.

one fourth of the spectrum and the peak amplitude of the recovered pulse has been degraded to  $\sim 60\%$  (see Fig. 4(f)). For case (iii) with five filters and a CS of 100 GHz, the peak amplitude of the decoded pulse can reach up to a similar level as case (ii), indicating that the notch filter used in this experiment can approximately emulate five DWDM channels. While for the multiple filters of case (iv), the maximum amplitude of the decoded pulse is  $\sim 20\%$  of the ideal one. It is worth noting from Figs. 4(f)–4(h) that the auto-correlation signal after notch filtering still presents as an optical pulse, but it has some small sidelobes, inducing phase noise in the DPSK signal and degradation of the BER performance. Figure 5 depicts the effect of filter bandwidth (centered at 1550.9 nm) on the decoding and BER performance for three different code patterns, from which one finds that, as the bandwidth of the notch filter increases to 3 nm, the normalized peak amplitude of the decoded pulse decays gradually from 1 to 0.1 and the corresponding BER degrades from  $10^{-9}$  to  $10^{-3}$  for codes 11101000 and 10010110. The other code 10101010 exhibits similar trends, but the peak amplitude and corresponding BER degrade more significantly than the others, which can be ascribed to the decoding performance discrepancy produced by the code transition of the pattern generator. In the experiment, the spectral notch filter has a bandwidth of 1 nm and is used to reject the two CW channels simultaneously, which can keep the peak amplitude and BER at an appropriate level. The dependence of the center wavelength of the notch filter on the BER and Q factor has also been simulated for code 11101000, as shown in Figs. 6(a) and 6(b), respectively. It can be seen that notch filtering at the left (1549.1 nm) and right (1550.9 nm) spectral edge (relative to the OCDM spectral center of 1549.9 nm) for 3 nm BW causes the BER performance and Q factor to degrade to about  $10^{-3}$  and 3, respectively, while for the notch filtering near the spectral center (1550 nm), the log(BER) and Q factor both rapidly degrade to 0 because the spectral center occupies most of the energy that induces more severe degradation, especially at larger filtering bandwidth. Due to the asymmetry of the encoded spectrum for code 11101000, notch filtering at the left and right spectra edge exhibit slightly different performances. To alleviate the degradation, a notch filter with a center wavelength of 1550.9 nm is employed in the experiment.

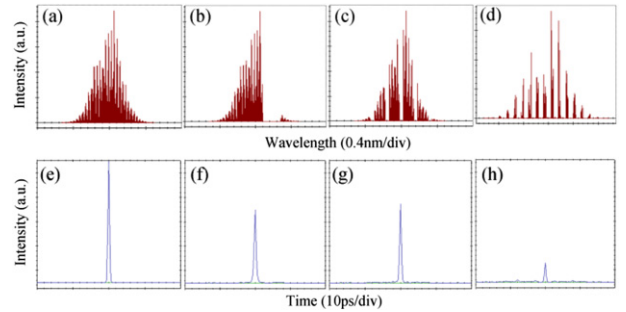


Fig. 4. (Color online) (a)–(d) and (e)–(h) are the encoded spectra and corresponding decoded waveforms with four different kinds of notch filters.

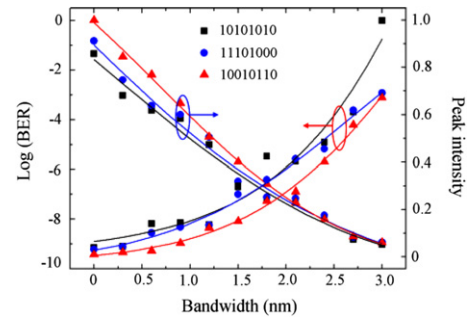


Fig. 5. (Color online) BER performance and peak amplitude of the decoded pulse versus the bandwidth of the notch filter for different codes.

#### IV. RESULTS AND DISCUSSION

Figures 7(a) and 7(b) show the spectrum and waveform of the stretched OCDM signal after the first LCFBG, from which one can see that the input broadband SC spectrum has been cut off by the LCFBG, resulting in a stretched pulse of time duration within one bit period of 400 ps, corresponding to an effective code length of 8 chips for a chip rate of 20 Gchips/s. By adjusting the optical attenuator after the PM, the DPSK data modulated SPE-OCODM signal can be combined with the two-channel DWDM signal with a power ratio of  $\sim 19$  dB for transmission. It can be seen from Fig. 7(c) that the secure OCDM channel occupies the same spectral bandwidth as



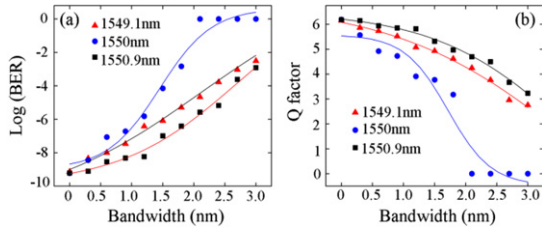


Fig. 6. (Color online) (a) BER performance and (b) Q factor versus the notch filtering bandwidth at different center wavelengths.

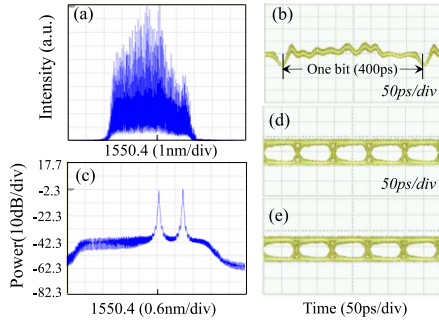


Fig. 7. (Color online) (a) and (b) are the spectrum and waveform of the OCDM signal after the LCFBG, (c) is the spectrum of the combined DWDM and OCDM signals, (d) and (e) are the eye diagrams for the DWDM signal without and with OCDM signal.

the DWDM signal; thus the OCDM/DWDM signals can be simultaneously processed during the transmission to improve the bandwidth efficiency. The peak power of the OCDM spectrum is approaching the system noise level, which is  $\sim 35$  dB lower than that of the DWDM channels. By injecting ASE noise into the system, the broadband OCDM spectrum could be further masked without significantly jeopardizing the public channel. The eye diagrams of the DWDM signals without and with OCDM signal are shown in Figs. 7(d) and 7(e), from which one can see a clear 10-Gb/s NRZ-OOK eye diagram. There is no obvious difference in the NRZ-OOK eye diagrams before and after introducing the OCDM signal that may make the eavesdropper unaware of the secure OCDM channel.

After the spectral notch filter with a notch depth of  $\sim 30$  dB, most of the DWDM signal has been rejected from the broadband OCDM spectrum and directly detected for both of the two different wavelengths, while the OCDM signal survives from the transmission port. To investigate the decoding performance of the OCDM signal after the notch filter, we have tried four optical codes OC1–OC4: 11101000, 10010110, 11011100, and 10101010 in the experiment. By properly applying the correct optical code sequence, the encoded SPE-OCDM signal can be spectrally phase decoded and compressed by the LCFBG to recover a pulse like the original with a different phase of 0 and  $\pi$ . Figure 8 shows the correctly decoded spectra (upper row) and recovered waveforms (middle row), from which one can see that compared with the case with only DPSK data (code 11111111), the decoded waveforms for the other codes have been slightly degraded. The corresponding eye diagrams of the 2.5-Gb/s DPSK–OCDM

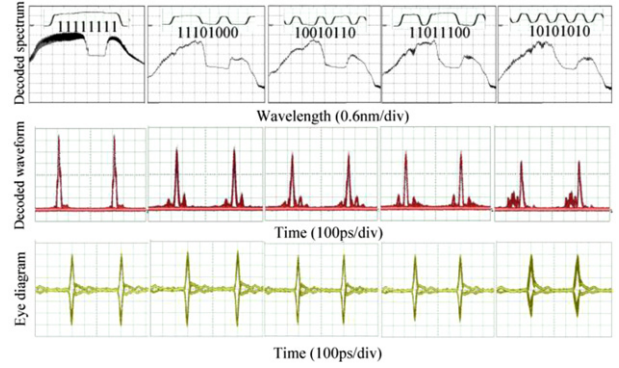


Fig. 8. (Color online) Decoded spectra after the notch filter (upper row), decoded waveforms (middle row), and corresponding eye diagrams (lower row) for different code patterns.

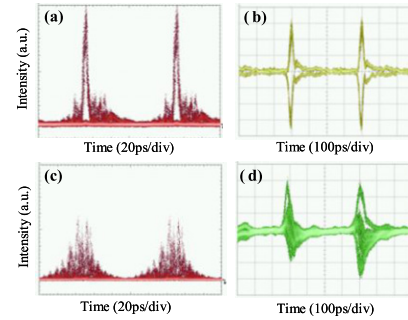


Fig. 9. (Color online) (a) and (b) are the waveform and corresponding eye diagram for the correctly decoded scrambled OCDM signal; (c) and (d) are the waveform and eye diagram for an incorrectly decoded signal.

signal with a clear eye opening are shown in the lower row of Fig. 8, which indicates that the phase information has been successfully retrieved. Note that the decoded waveform and eye diagram for the code 10101010 has deteriorated significantly more than the other codes due to the frequent change of the chip patterns with rise and fall transitions generated by the pulse pattern generator that cause the phase mismatch between the en/decoding side during the code transition time.

To further improve the security of the OCDM signal, we have applied a prime hopping code pattern comprised of the three codes OC1–OC3 to modulate the phase of the stretched optical signal: for a series of data streams, each bit of the optical pulse can be encoded bit-by-bit by scrambling the code patterns. For instance, the PM can be driven by the code sequence of OC3, OC1, OC2, OC1, OC3, ... for encoding. To combine the DPSK data (e.g., 10010) with the code pattern, the PM is driven by OC as follows: when the DPSK data is symbol “1,” the PM is driven by OC, whereas if the symbol is “0,” the PM is driven by  $\overline{\text{OC}}$ , so the data stream can be coded by OC3,  $\overline{\text{OC1}}$ ,  $\overline{\text{OC2}}$ , OC1, OC3 for enhancing the security.

To decode the SPE-OCDM signal, the PM in the SPD section should be driven only by the complementary scrambled code patterns  $\overline{\text{OC3}}$ ,  $\overline{\text{OC1}}$ ,  $\overline{\text{OC2}}$ , OC1, OC3, ... to generate an auto-correlation pulse stream with high peak intensity; otherwise a cross-correlation signal with low peak power will be produced. Synchronization between the transmitter and

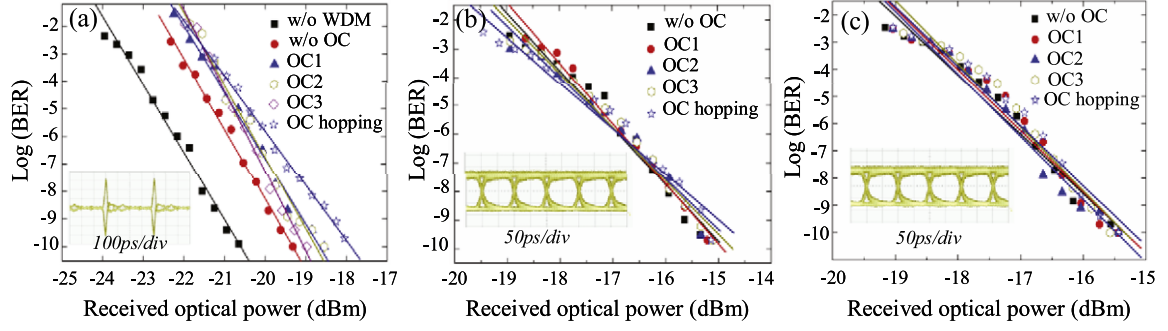


Fig. 10. (a) BER performances for the OCDM signal with different codes; (b) and (c) are the BER performances of WDM channels 1 and 2, respectively.

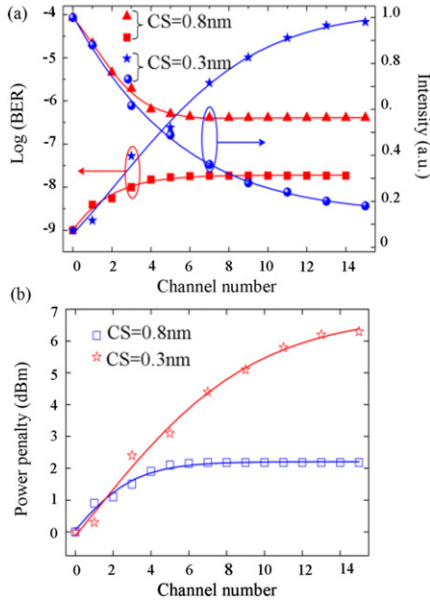


Fig. 11. (Color online) (a) BER performance and normalized intensity versus channel number for a CS of 0.8 nm and 0.3 nm, respectively; (b) power penalty versus channel number.

receiver side is essential for decoding and improving the security, which can be achieved by a tunable optical delay line with a long tuning range and chip-level resolution for precise adjustment in the experiment. Figures 9(a) and 9(b) show the correctly decoded optical signal measured by a 10 GHz optical sampling oscilloscope and its corresponding electrical eye diagram, both of which exhibit a clear eye opening. In contrast, an eavesdropper can only get an obscure eye diagram and it is not easy to break the security of the OCDM channel without the knowledge of the scrambled code pattern, as can be seen from the decoded optical waveform and eye diagram of the cross-correlation signals, which behave as noise in Figs. 9(c)–9(d). By increasing the chip length, the security of the OCDM signal can be further enhanced.

Finally, we have measured the BER after 49 km transmission for the correctly decoded OCDM signal as shown in Fig. 10(a). Error-free transmission has been achieved for all three codes, and the average power penalty is about 2 dB compared to that of no WDM/notch filter. As shown in

Fig. 10(a), by using a correct code hopping sequence to drive the PM, the scrambled OCDM signal can also be decoded and error-free transmitted with low penalty. Figures 10(b) and 10(c) show the measured BER for the two WDM channels in the presence of the OCDM signal with different codes, respectively. A BER lower than  $10^{-9}$  for both the WDM channels has been obtained and no power penalty was observed for different codes. In the experiment, the power ratio of the two-channel WDM and OCDM signals is  $\sim 19$  dB, which can be further increased as long as the notch depth of the filter is high enough. It is also possible to get error-free detection of the OCDM and DWDM signals in the hybrid system with multiple channels to improve the bandwidth efficiency and security. Figure 11(a) shows the calculated BER performance and peak amplitude via the OptiSystem software for two kinds of notch filters with a BW of 0.2 nm and different CS: one is ITU-T DWDM grid 0.8 nm, and the other is 0.3 nm. For the CS of 0.8 nm, as the channel number increases to 5, the peak amplitude gradually decreases from 1 to 0.6, and the corresponding BER has been degraded from  $10^{-9}$  to  $10^{-8}$ . For channel numbers greater than 5, the peak intensity and BER will remain stable because the residual channels are out of the OCDM bandwidth, whereas for denser channels of 0.3 nm spacing, the peak intensity and BER degrade rapidly with the channel numbers. The required additional power to compensate the peak intensity reduction is shown in Fig. 11(b), from which one can see that the maximum power penalty due to the notch filtering is about 2 dB and 6 dB for the CS of 0.8 nm and 0.3 nm, which indicates the feasibility of error-free detecting the OCDM and DWDM signal with low power penalty in the OCDM overlay DWDM network.

## V. CONCLUSION

We have experimentally demonstrated the transparent transmission and detection of a secure 2.5-Gb/s DPSK–OCDM channel spectrally overlaid on a two-channel 10-Gb/s DWDM network enabled by a spectral notch filter. With the public DWDM channels, it is difficult for an eavesdropper to be aware of the existence of the secure OCDM channel. A time domain spectral phase encoding/decoding scheme that can simultaneously generate DPSK data modulation and even bit-by-bit optical code scrambling has also been applied to the secure OCDM channel to significantly improve the data confidentiality. Error-free transmission of the DPSK–OCDM

and two-channel DWDM signals over 49 km has been successfully achieved, which verifies the network transparency of such an OCDM overlay DWDM system and the potential to apply this technique to higher data rates and multiple channels with low power penalty to achieve high system security and capacity.

## REFERENCES

- [1] A. Stok and E. H. Sargent, "The role of optical CDMA in access networks," *IEEE Commun. Mag.*, vol. 40, no. 9, pp. 83–87, 2002.
- [2] J. P. Heritage and A. M. Weiner, "Advances in spectral optical code-division multiple-access," *IEEE J. Quantum Electron.*, vol. 13, no. 5, pp. 1351–1369, 2007.
- [3] T. H. Shake, "Confidentiality performance of spectral-phase-encoded optical CDMA," *J. Lightwave Technol.*, vol. 23, no. 4, pp. 1652–1663, 2005.
- [4] X. Wang and K. Kitayama, "Analysis of beat noise in coherent and incoherent time-spreading OCDMA," *J. Lightwave Technol.*, vol. 22, no. 10, pp. 2226–2235, 2004.
- [5] R. J. Essiambre, G. J. Foschini, G. Kramer, and P. J. Winzer, "Capacity limits of information transport in fiber-optic networks," *Phys. Rev. Lett.*, vol. 101, 163901, 2008.
- [6] J. Kani, K. Iwatsuki, and T. Imai, "Optical multiplexing technologies for access area applications," *IEEE J. Sel. Top. Quantum Electron.*, vol. 12, no. 4, pp. 661–668, 2006.
- [7] K. Kitayama, X. Wang, and N. Wada, "OCDMA over WDM PON-solution path to gigabit-symmetric FTTH," *J. Lightwave Technol.*, vol. 24, no. 4, pp. 1654–1662, 2006.
- [8] S. Galli, R. Menendez, P. Toliver, T. Banwell, J. Jackel, J. Young, and S. Etemad, "Experimental results on the simultaneous transmission of two 2.5 Gbps optical-CDMA channels and a 10 Gbps OOK channel within the same WDM window," in *Optical Fiber Communication Conf. and Expo. and the Nat. Fiber Optic Engineers Conf.*, 2005, OWB3.
- [9] S. Galli, R. Menendez, P. Toliver, T. Banwell, J. Jackel, J. Young, and S. Etemad, "DWDM-compatible spectrally phase encoded O-CDMA," in *IEEE Global Telecommunications Conf. (GLOBE-COM)*, Dallas, TX, USA, 2004, pp. 1888–1894.
- [10] S. Galli, R. Menendez, P. Toliver, T. Banwell, J. Jackel, J. Young, and S. Etemad, "Novel results on the coexistence of spectrally phase encoded OCDMA and DWDM," in *IEEE Int. Conf. on Communications (ICC)*, Seoul, South Korea, May 16–20, 2005, pp. 1608–1612.
- [11] M. Yoshino, N. Miki, N. Yoshimoto, and M. Tsubokawa, "Simultaneous OCDM signal transmission over multiple WDM channels using Mach-Zehnder interferometric selector," *Electron. Lett.*, vol. 44, no. 22, pp. 1319–1320, 2008.
- [12] K. Kravtsov, B. Wu, I. Glesk, P. R. Prucnal, and E. Narimanov, "Stealth transmission over a WDM network with detection based on an all-optical threshold," in *IEEE/LEOS Annual Meeting*, 2007, pp. 480–481.
- [13] B. Wu, P. R. Prucnal, and E. E. Narimanov, "Secure transmission over an existing public WDM lightwave network," *IEEE Photon. Technol. Lett.*, vol. 18, no. 17, pp. 1870–1872, 2006.
- [14] B. B. Wu and E. E. Narimanov, "A method for secure communications over a public fiber-optical network," *Opt. Express*, vol. 14, no. 9, pp. 3738–3751, 2006.
- [15] X. Hong, D. Wang, L. Xu, and S. He, "Demonstration of optical steganography transmission using temporal phase coded optical signals with spectral notch filtering," *Opt. Express*, vol. 18, no. 12, pp. 12415–12420, 2010.
- [16] Z. Wang and P. R. Prucnal, "Optical steganography over public DPSK channel with asynchronous detection," *IEEE Photon. Technol. Lett.*, vol. 23, no. 1, pp. 48–50, 2011.
- [17] H. Sotobayashi, W. Chujo, and K. Kitayama, "Transparent virtual optical code/wavelength path network," *IEEE J. Sel. Areas Commun.*, vol. 8, no. 3, pp. 699–704, May 2002.
- [18] X. Wang and N. Wada, "Spectral phase encoding of ultra-short optical pulse in time domain for OCDMA application," *Opt. Express*, vol. 15, no. 12, pp. 7319–7326, 2007.
- [19] V. J. Hernandez, Y. Du, W. Cong, R. P. Scott, K. Li, J. P. Heritage, Z. Ding, B. H. Kolner, and S. J. Ben Yoo, "Spectral phase-encoded time spreading (SPECTS) optical code-division multiple access for terabit optical access networks," *J. Lightwave Technol.*, vol. 22, no. 11, pp. 2671–2679, 2004.
- [20] X. Wang, Z. Gao, N. Kataoka, and N. Wada, "Time domain spectral phase encoding/DPSK data modulation using single phase modulator for OCDMA application," *Opt. Express*, vol. 18, no. 10, pp. 9879–9890, 2010.

**Zhensen Gao** (S'10) received the B.S. and M.S. degrees in the Department of Physics from Harbin Institute of Technology, Harbin, China, in 2006 and 2008, respectively. He is currently working towards the Ph.D. degree in the Department of Electrical, Electronic & Computer Engineering, Heriot-Watt University, UK.

**Bo Dai** (S'10) received the B.Eng. (Hon.I) degree in the Department of Electronic Engineering from City University of Hong Kong in 2009. He is currently pursuing the Ph.D. degree in the Department of Electrical, Electronic & Computer Engineering, Heriot-Watt University, UK.

**Xu Wang** (S'91–M'98–SM'06) received the B.S. degree in physics from Zhejiang University, Hangzhou, China, in 1989; the M.S. degree in electronics engineering from the University of Electronics Science and Technology of China (UESTC), Chengdu, China, in 1992; and the Ph.D. degree in electronics engineering from the Chinese University of Hong Kong (CUHK) in 2001. He is currently a Senior Lecturer in the School of Engineering and Physical Sciences, Heriot-Watt University, Edinburgh, UK. His research interests include fiber-optical networks, optical-code-division multiplexing, optical packet switching, and optic signal processing.

**Nobuyuki Kataoka** (S'03–M'06) received the B.E., M.E. and Dr.Eng. degrees from Osaka University, Osaka, Japan, in 2001, 2003, and 2006, respectively. In 2006, he joined the National Institute of Information and Communications Technology (NICT), Tokyo, Japan. His research interests are in the area of photonic networks such as optical packet switching, optical add/drop multiplexing, and optical-code-division multiple access.

**Naoya Wada** (M'97) received the B.E., M.E., and Dr.Eng. degrees in electronics from Hokkaido University, Sapporo, Japan, in 1991, 1993, and 1996, respectively. Since 2006, he has been the research manager of the Photonic Network Group in the National Institute of Information and Communications Technology (NICT), Tokyo, Japan. His current research interests are in the area of photonic networks and optical communication technologies, such as optical packet switching (OPS) networks and optical-code-division multiple access (OCDMA) systems.